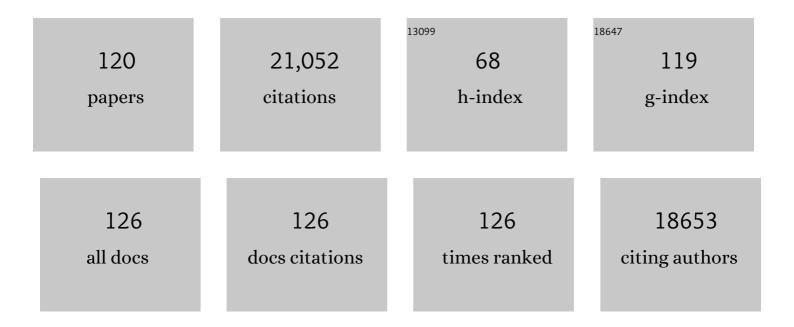
List of Publications by Year in descending order

Source: https://exaly.com/author-pdf/9362769/publications.pdf Version: 2024-02-01



#	Article	IF	CITATIONS
1	Polymeric Photocatalysts Based on Graphitic Carbon Nitride. Advanced Materials, 2015, 27, 2150-2176.	21.0	3,046
2	2D/2D Heterojunction of Ultrathin MXene/Bi <sub>2</sub> WO <sub>6</sub> Nanosheets for Improved Photocatalytic CO <sub>2</sub> Reduction. Advanced Functional Materials, 2018, 28, 1800136.	14.9	1,157
3	g-C <sub>3</sub> N <sub>4</sub> -Based Photocatalysts for Hydrogen Generation. Journal of Physical Chemistry Letters, 2014, 5, 2101-2107.	4.6	1,107
4	Designing a 0D/2D Sâ€Scheme Heterojunction over Polymeric Carbon Nitride for Visibleâ€Light Photocatalytic Inactivation of Bacteria. Angewandte Chemie - International Edition, 2020, 59, 5218-5225.	13.8	822
5	Ultra-thin nanosheet assemblies of graphitic carbon nitride for enhanced photocatalytic CO <sub>2</sub> reduction. Journal of Materials Chemistry A, 2017, 5, 3230-3238.	10.3	621
6	Size- and shape-dependent catalytic performances of oxidation and reduction reactions on nanocatalysts. Chemical Society Reviews, 2016, 45, 4747-4765.	38.1	568
7	Two-dimensional layered composite photocatalysts. Chemical Communications, 2014, 50, 10768.	4.1	551
8	An Inorganic/Organic Sâ€5cheme Heterojunction H <sub>2</sub> â€Production Photocatalyst and its Charge Transfer Mechanism. Advanced Materials, 2021, 33, e2100317.	21.0	528
9	Enhanced photocatalytic activity and stability of Z-scheme Ag2CrO4-GO composite photocatalysts for organic pollutant degradation. Applied Catalysis B: Environmental, 2015, 164, 380-388.	20.2	483
10	Recent advances in visible light Bi-based photocatalysts. Chinese Journal of Catalysis, 2014, 35, 989-1007.	14.0	481
11	Monodisperse α-Fe2O3 Mesoporous Microspheres: One-Step NaCl-Assisted Microwave-Solvothermal Preparation, Size Control and Photocatalytic Property. Nanoscale Research Letters, 2011, 6, 1.	5.7	452
12	Solar-to-fuels conversion over In2O3/g-C3N4 hybrid photocatalysts. Applied Catalysis B: Environmental, 2014, 147, 940-946.	20.2	398
13	Semiconductor-based photocatalytic CO <sub>2</sub> conversion. Materials Horizons, 2015, 2, 261-278.	12.2	380
14	In-situ growth of CdS quantum dots on g-C3N4 nanosheets for highly efficient photocatalytic hydrogen generation under visible light irradiation. International Journal of Hydrogen Energy, 2013, 38, 1258-1266.	7.1	339
15	Facet effect of Pd cocatalyst on photocatalytic CO 2 reduction over g-C 3 N 4. Journal of Catalysis, 2017, 349, 208-217.	6.2	332
16	Hierarchically Nanostructured Magnetic Hollow Spheres of Fe <sub>3</sub> O <sub>4</sub> and γ-Fe <sub>2</sub> O <sub>3</sub> :  Preparation and Potential Application in Drug Delivery. Journal of Physical Chemistry C, 2008, 112, 1851-1856.	3.1	328
17	TiO2 nanosheets with exposed {001} facets for photocatalytic applications. Nano Research, 2016, 9, 3-27.	10.4	327
18	Singleâ€Atom Engineering of Directional Charge Transfer Channels and Active Sites for Photocatalytic Hydrogen Evolution. Advanced Functional Materials, 2018, 28, 1802169.	14.9	287

#	Article	IF	CITATIONS
19	Au/Pt Nanoparticle-Decorated TiO <sub>2</sub> Nanofibers with Plasmon-Enhanced Photocatalytic Activities for Solar-to-Fuel Conversion. Journal of Physical Chemistry C, 2013, 117, 25939-25947.	3.1	277
20	Hierarchically Nanostructured α-Fe <sub>2</sub> O <sub>3</sub> Hollow Spheres:  Preparation, Growth Mechanism, Photocatalytic Property, and Application in Water Treatment. Journal of Physical Chemistry C, 2008, 112, 6253-6257.	3.1	272
21	Preparation of Au-BiVO <sub>4</sub> Heterogeneous Nanostructures as Highly Efficient Visible-Light Photocatalysts. ACS Applied Materials & Interfaces, 2012, 4, 418-423.	8.0	259
22	Designing Defective Crystalline Carbon Nitride to Enable Selective CO <sub>2</sub> Photoreduction in the Gas Phase. Advanced Functional Materials, 2019, 29, 1900093.	14.9	254
23	Improving photocatalytic hydrogen production of metal–organic framework UiO-66 octahedrons by dye-sensitization. Applied Catalysis B: Environmental, 2015, 168-169, 572-576.	20.2	252
24	Carbon-based H2-production photocatalytic materials. Journal of Photochemistry and Photobiology C: Photochemistry Reviews, 2016, 27, 72-99.	11.6	252
25	A comparison study of alkali metal-doped g-C3N4 for visible-light photocatalytic hydrogen evolution. Chinese Journal of Catalysis, 2017, 38, 1981-1989.	14.0	244
26	g-C3N4 modified TiO2 nanosheets with enhanced photoelectric conversion efficiency in dye-sensitized solar cells. Journal of Power Sources, 2015, 274, 77-84.	7.8	241
27	Efficient photocatalytic reduction of CO2 by amine-functionalized g-C3N4. Applied Surface Science, 2015, 358, 350-355.	6.1	229
28	Red phosphor/g-C3N4 heterojunction with enhanced photocatalytic activities for solar fuels production. Applied Catalysis B: Environmental, 2013, 140-141, 164-168.	20.2	219
29	Structure effect of graphene on the photocatalytic performance of plasmonic Ag/Ag2CO3-rGO for photocatalytic elimination of pollutants. Applied Catalysis B: Environmental, 2016, 181, 71-78.	20.2	219
30	Trace-level phosphorus and sodium co-doping of g-C 3 N 4 for enhanced photocatalytic H 2 production. Journal of Power Sources, 2017, 351, 151-159.	7.8	205
31	Shape-dependent photocatalytic hydrogen evolution activity over a Pt nanoparticle coupled g-C <sub>3</sub> N <sub>4</sub> photocatalyst. Physical Chemistry Chemical Physics, 2016, 18, 19457-19463.	2.8	190
32	Highly Selective CO2 Capture and Its Direct Photochemical Conversion on Ordered 2D/1D Heterojunctions. Joule, 2019, 3, 2792-2805.	24.0	189
33	Advances in designing heterojunction photocatalytic materials. Chinese Journal of Catalysis, 2021, 42, 710-730.	14.0	182
34	Au@TiO <sub>2</sub> –CdS Ternary Nanostructures for Efficient Visible-Light-Driven Hydrogen Generation. ACS Applied Materials & Interfaces, 2013, 5, 8088-8092.	8.0	177
35	Noble-metal-free g-C3N4/Ni(dmgH)2 composite for efficient photocatalytic hydrogen evolution under visible light irradiation. Applied Surface Science, 2014, 319, 344-349.	6.1	169
36	Au/PtO nanoparticle-modified g-C 3 N 4 for plasmon-enhanced photocatalytic hydrogen evolution under visible light. Journal of Colloid and Interface Science, 2016, 461, 56-63.	9.4	169

#	Article	IF	CITATIONS
37	Nanostructured porous hollow ellipsoidal capsules of hydroxyapatite and calcium silicate: preparation and application in drug delivery. Journal of Materials Chemistry, 2008, 18, 2722.	6.7	166
38	Microwave-assisted heating synthesis: a general and rapid strategy for large-scale production of highly crystalline g-C <sub>3</sub> N <sub>4</sub> with enhanced photocatalytic H <sub>2</sub> production. Green Chemistry, 2014, 16, 4663-4668.	9.0	166
39	A Single Cu-Center Containing Enzyme-Mimic Enabling Full Photosynthesis under CO <sub>2</sub> Reduction. ACS Nano, 2020, 14, 8584-8593.	14.6	166
40	Mesoporous plasmonic Au–TiO2 nanocomposites for efficient visible-light-driven photocatalytic water reduction. International Journal of Hydrogen Energy, 2012, 37, 17853-17861.	7.1	151
41	ZnFe2O4 nanoparticles: Microwave-hydrothermal ionic liquid synthesis and photocatalytic property over phenol. Journal of Hazardous Materials, 2009, 171, 431-435.	12.4	149
42	Direct evidence of plasmon enhancement on photocatalytic hydrogen generation over Au/Pt-decorated TiO <sub>2</sub> nanofibers. Nanoscale, 2014, 6, 5217-5222.	5.6	143
43	Hierachically Nanostructured Mesoporous Spheres of Calcium Silicate Hydrate: Surfactantâ€Free Sonochemical Synthesis and Drugâ€Delivery System with Ultrahigh Drug‣oading Capacity. Advanced Materials, 2010, 22, 749-753.	21.0	142
44	Cu2(OH)2CO3 clusters: Novel noble-metal-free cocatalysts for efficient photocatalytic hydrogen production from water splitting. Applied Catalysis B: Environmental, 2017, 205, 104-111.	20.2	137
45	Enhanced visible-light-driven photocatalytic hydrogen generation over g-C3N4 through loading the noble metal-free NiS2 cocatalyst. RSC Advances, 2014, 4, 6127.	3.6	136
46	Surfactant-Free Preparation and Drug Release Property of Magnetic Hollow Core/Shell Hierarchical Nanostructures. Journal of Physical Chemistry C, 2008, 112, 12149-12156.	3.1	118
47	Gold Coating of Silver Nanoprisms. Advanced Functional Materials, 2012, 22, 849-854.	14.9	116
48	Selective photocatalytic decomposition of formic acid over AuPd nanoparticle-decorated TiO 2 nanofibers toward high-yield hydrogen production. Applied Catalysis B: Environmental, 2015, 162, 204-209.	20.2	107
49	Enhanced photocatalytic CO2-reduction activity of electrospun mesoporous TiO2 nanofibers by solvothermal treatment. Dalton Transactions, 2014, 43, 9158.	3.3	105
50	Iron oxide hollow spheres: Microwave–hydrothermal ionic liquid preparation, formation mechanism, crystal phase and morphology control and properties. Acta Materialia, 2009, 57, 2154-2165.	7.9	104
51	Large impact of heating time on physical properties and photocatalytic H2 production of g-C3N4 nanosheets synthesized through urea polymerization in Ar atmosphere. International Journal of Hydrogen Energy, 2013, 38, 13159-13163.	7.1	103
52	Artificial photosynthetic hydrogen evolution over g-C3N4 nanosheets coupled with cobaloxime. Physical Chemistry Chemical Physics, 2013, 15, 18363.	2.8	101
53	Microwave-assisted solvothermal synthesis of Bi4O5I2 hierarchical architectures with high photocatalytic performance. Catalysis Today, 2016, 264, 221-228.	4.4	100
54	Hierarchical hollow cages of Mn-Co layered double hydroxide as supercapacitor electrode materials. Applied Surface Science, 2017, 413, 35-40.	6.1	98

#	Article	IF	CITATIONS
55	Efficient CO <sub>2</sub> Capture and Photoreduction by Amineâ€Functionalized TiO <sub>2</sub> . Chemistry - A European Journal, 2014, 20, 10220-10222.	3.3	95
56	Promoting intramolecular charge transfer of graphitic carbon nitride by donor–acceptor modulation for visibleâ€light photocatalytic H <sub>2</sub> evolution. , 2022, 1, 294-308.		92
57	From Millimeter to Subnanometer: Vapor–Solid Deposition of Carbon Nitride Hierarchical Nanostructures Directed by Supramolecular Assembly. Angewandte Chemie - International Edition, 2017, 56, 8426-8430.	13.8	90
58	Supramolecular Chemistry in Molten Sulfur: Preorganization Effects Leading to Marked Enhancement of Carbon Nitride Photoelectrochemistry. Advanced Functional Materials, 2015, 25, 6265-6271.	14.9	89
59	Fe3O4 polyhedral nanoparticles with a high magnetization synthesized in mixed solvent ethylene glycol–water system. New Journal of Chemistry, 2008, 32, 1526.	2.8	86
60	Dual Z-scheme charge transfer in TiO2–Ag–Cu2O composite for enhanced photocatalytic hydrogen generation. Journal of Materiomics, 2015, 1, 124-133.	5.7	86
61	Recent Advances in Morphology Control and Surface Modification of Bi-Based Photocatalysts. Wuli Huaxue Xuebao/ Acta Physico - Chimica Sinica, 2016, 32, 2841-2870.	4.9	85
62	Controlling defects in crystalline carbon nitride to optimize photocatalytic CO <sub>2</sub> reduction. Chemical Communications, 2020, 56, 5641-5644.	4.1	83
63	Nanoparticle heterojunctions in ZnS–ZnO hybrid nanowires for visible-light-driven photocatalytic hydrogen generation. CrystEngComm, 2013, 15, 5688.	2.6	77
64	NiS2 Co-catalyst decoration on CdLa2S4 nanocrystals for efficient photocatalytic hydrogen generation under visible light irradiation. International Journal of Hydrogen Energy, 2013, 38, 7218-7223.	7.1	76
65	Effects of the preparation method on the structure and the visible-light photocatalytic activity of Ag <sub>2</sub> CrO <sub>4</sub> . Beilstein Journal of Nanotechnology, 2014, 5, 658-666.	2.8	76
66	3D BiOl–GO composite with enhanced photocatalytic performance for phenol degradation under visible-light. Ceramics International, 2015, 41, 3511-3517.	4.8	74
67	Room-temperature synthesis of BiOI with tailorable (0 0 1) facets and enhanced photocatalytic activity. Journal of Colloid and Interface Science, 2016, 478, 201-208.	9.4	74
68	Ni-P cluster modified carbon nitride toward efficient photocatalytic hydrogen production. Chinese Journal of Catalysis, 2019, 40, 867-874.	14.0	73
69	Molecule-Based Water-Oxidation Catalysts (WOCs): Cluster-Size-Dependent Dye-Sensitized Polyoxometalates for Visible-Light-Driven O2 Evolution. Scientific Reports, 2013, 3, 1853.	3.3	69
70	Surfactantâ€Free Subâ€2 nm Ultrathin Triangular Gold Nanoframes. Small, 2013, 9, 2880-2886.	10.0	66
71	Synthesis of Organized Layered Carbon by Selfâ€Templating of Dithiooxamide. Advanced Materials, 2016, 28, 6727-6733.	21.0	59
72	Improving Artificial Photosynthesis over Carbon Nitride by Gas–Liquid–Solid Interface Management for Full Lightâ€Induced CO <sub>2</sub> Reduction to C <sub>1</sub> and C <sub>2</sub> Fuels and O <sub>2</sub> . ChemSusChem, 2020, 13, 1730-1734.	6.8	59

#	Article	IF	CITATIONS
73	Vectorial doping-promoting charge transfer in anatase TiO2 {001} surface. Applied Surface Science, 2014, 319, 167-172.	6.1	55
74	Enhanced photochemical CO <sub>2</sub> reduction in the gas phase by graphdiyne. Journal of Materials Chemistry A, 2020, 8, 7671-7676.	10.3	52
75	A strategy for in-situ synthesis of well-defined core–shell Au@TiO2 hollow spheres for enhanced photocatalytic hydrogen evolution. Chemical Engineering Journal, 2014, 257, 112-121.	12.7	51
76	In situ growth of Au nanoparticles on Fe2O3 nanocrystals for catalytic applications. CrystEngComm, 2012, 14, 7229.	2.6	48
77	Calcium phosphate drug nanocarriers with ultrahigh and adjustable drug-loading capacity: One-step synthesis, in situ drug loading and prolonged drug release. Nanomedicine: Nanotechnology, Biology, and Medicine, 2011, 7, 428-434.	3.3	47
78	Ionâ€Induced Synthesis of Uniform Singleâ€Crystalline Sulphideâ€Based Quaternaryâ€Alloy Hexagonal Nanorings for Highly Efficient Photocatalytic Hydrogen Evolution. Advanced Materials, 2013, 25, 2567-2572.	21.0	45
79	Dependence of Exposed Facet of Pd on Photocatalytic H <sub>2</sub> -Production Activity. ACS Sustainable Chemistry and Engineering, 2018, 6, 6478-6487.	6.7	41
80	Plasmon-Enhanced Hydrogen Evolution on Au-InVO4 Hybrid Microspheres. RSC Advances, 2012, 2, 5513.	3.6	40
81	Preparation and Sustained-Release Property of Triblock Copolymer/Calcium Phosphate Nanocomposite as Nanocarrier for Hydrophobic Drug. Nanoscale Research Letters, 2010, 5, 781-785.	5.7	38
82	Rapid microwave-assisted synthesis and characterization of cellulose-hydroxyapatite nanocomposites in N,N-dimethylacetamide solvent. Carbohydrate Research, 2010, 345, 1046-1050.	2.3	38
83	Nanocages of Polymeric Carbon Nitride from Lowâ€Temperature Supramolecular Preorganization for Photocatalytic CO <sub>2</sub> Reduction. Solar Rrl, 2020, 4, 1900469.	5.8	38
84	Porous nanocomposites of PEG-PLA/calcium phosphate: room-temperature synthesis and its application in drug delivery. Dalton Transactions, 2010, 39, 4435.	3.3	37
85	Solar-Driven Glucose Isomerization into Fructose via Transient Lewis Acid–Base Active Sites. ACS Catalysis, 2021, 11, 12170-12178.	11.2	36
86	Preparation and photocatalytic property of α-Fe2O3 hollow core/shell hierarchical nanostructures. Journal of Physics and Chemistry of Solids, 2010, 71, 1680-1683.	4.0	33
87	Effect of sacrificial agents on the dispersion of metal cocatalysts for photocatalytic hydrogen evolution. Applied Surface Science, 2018, 442, 361-367.	6.1	33
88	"Environmental phosphorylation―boosting photocatalytic CO2 reduction over polymeric carbon nitride grown on carbon paper at air-liquid-solid joint interfaces. Chinese Journal of Catalysis, 2021, 42, 1667-1676.	14.0	33
89	Formation of γ-Fe2O3 hierarchical nanostructures at 500°C in a high magnetic field. Journal of Magnetism and Magnetic Materials, 2009, 321, 3057-3060.	2.3	31
90	Ultra-Thin Carbon-Doped Bi2WO6 Nanosheets for Enhanced Photocatalytic CO2 Reduction. Transactions of Tianjin University, 2021, 27, 338-347.	6.4	29

#	Article	IF	CITATIONS
91	Light-driven directional ion transport for enhanced osmotic energy harvesting. National Science Review, 2021, 8, nwaa231.	9.5	24
92	Ultrathin 2D/2D Graphdiyne/Bi <sub>2</sub> WO <sub>6</sub> Heterojunction for Gas-Phase CO <sub>2</sub> Photoreduction. ACS Applied Energy Materials, 2021, 4, 8734-8738.	5.1	23
93	Rational Synthesis of Triangular Au–Ag <sub>2</sub> S Hybrid Nanoframes with Effective Photoresponses. Chemistry - A European Journal, 2014, 20, 2742-2745.	3.3	22
94	A "uniform―heterogeneous photocatalyst: integrated p–n type CuInS <sub>2</sub> /NaInS <sub>2</sub> nanosheets by partial ion exchange reaction for efficient H <sub>2</sub> evolution. Chemical Communications, 2015, 51, 9381-9384.	4.1	22
95	Calcium phosphate/block copolymer hybrid porous nanospheres: Preparation and application in drug delivery. Materials Letters, 2010, 64, 2299-2301.	2.6	21
96	A New Conducting Polymer with Exceptional Visible‣ight Photocatalytic Activity Derived from Barbituric Acid Polycondensation. Advanced Materials, 2020, 32, e1907702.	21.0	20
97	All-organic Z-scheme photoreduction of CO2 with water as the donor of electrons and protons. Applied Catalysis B: Environmental, 2021, 285, 119773.	20.2	19
98	Dye-sensitized Pt@TiO <sub>2</sub> core–shell nanostructures for the efficient photocatalytic generation of hydrogen. Beilstein Journal of Nanotechnology, 2014, 5, 360-364.	2.8	18
99	Potassium/oxygen co-doped polymeric carbon nitride for enhanced photocatalytic CO2 reduction. Applied Surface Science, 2021, 563, 150310.	6.1	18
100	Iron hydroxyl phosphate microspheres: Microwave-solvothermal ionic liquid synthesis, morphology control, and photoluminescent properties. Journal of Solid State Chemistry, 2010, 183, 1704-1709.	2.9	16
101	From Millimeter to Subnanometer: Vapor–Solid Deposition of Carbon Nitride Hierarchical Nanostructures Directed by Supramolecular Assembly. Angewandte Chemie, 2017, 129, 8546-8550.	2.0	16
102	MnCo Oxides Supported on Carbon Fibers for High-Performance Supercapacitors. Wuli Huaxue Xuebao/ Acta Physico - Chimica Sinica, 2020, 36, 1907072-0.	4.9	16
103	Dual synergetic catalytic effects boost hydrogen electric oxidation performance of Pd/W18O49. Nano Research, 2021, 14, 2441-2450.	10.4	15
104	An electrochemically reconstructed WC/WO <sub>2</sub> –WO <sub>3</sub> heterostructure as a highly efficient hydrogen oxidation electrocatalyst. Journal of Materials Chemistry A, 2022, 10, 622-631.	10.3	15
105	Hydrothermal synthesis of relatively uniform CePO4@LaPO4 one-dimensional nanostructures with highly improved luminescence. Journal of Alloys and Compounds, 2010, 492, 559-563.	5.5	14
106	Two-dimensional gersiloxenes with tunable band gap as new photocatalysts. Rare Metals, 2020, 39, 610-612.	7.1	14
107	Designing a 0D/2D S‣cheme Heterojunction over Polymeric Carbon Nitride for Visibleâ€Light Photocatalytic Inactivation of Bacteria. Angewandte Chemie, 2020, 132, 5256-5263.	2.0	14
108	A 3D Hierarchical Ti <sub>3</sub> C <sub>2</sub> T <sub>x</sub> /TiO <sub>2</sub> Heterojunction for Enhanced Photocatalytic CO <sub>2</sub> Reduction. ChemNanoMat, 2021, 7, 910-915.	2.8	14

#	Article	IF	CITATIONS
109	Donor–Acceptor Modification of Carbon Nitride for Enhanced Photocatalytic Hydrogen Evolution. Advanced Sustainable Systems, 2023, 7, .	5.3	14
110	Corrosion mechanism of E-glass of chemical resistance glass fiber in acid environment. Journal Wuhan University of Technology, Materials Science Edition, 2016, 31, 872-876.	1.0	13
111	Preparation and Drug Release Properties of Nanostructured CaCO <sub>3</sub> Porous Hollow Microspheres. Wuji Cailiao Xuebao/Journal of Inorganic Materials, 2009, 24, 166-170.	1.3	10
112	2D/2D FeNi-LDH/g-C <sub>3</sub> N <sub>4</sub> Hybrid Photocatalyst for Enhanced CO <sub>2</sub> Photoreduction. Wuli Huaxue Xuebao/ Acta Physico - Chimica Sinica, 2020, .	4.9	10
113	Development and Fabrication of Advanced Materials for Energy and Environment Applications. Journal of Nanomaterials, 2013, 2013, 1-2.	2.7	8
114	CsPbBr3 perovskite based tandem device for CO2 photoreduction. Chemical Engineering Journal, 2022, 443, 136447.	12.7	8
115	SnO2 and ZnO Nanostructured Spheres Self-assembled by Nanocrystals: Microwave-assisted Preparation and Enhancement of Photocatalytic Activity. Chemistry Letters, 2008, 37, 1002-1003.	1.3	7
116	Photocatalysis: Single-Atom Engineering of Directional Charge Transfer Channels and Active Sites for Photocatalytic Hydrogen Evolution (Adv. Funct. Mater. 32/2018). Advanced Functional Materials, 2018, 28, 1870224.	14.9	6
117	Preparation, Characterization and Application of Hollow Microspheres Assembled with Nanocrystals of Iron Oxides. Wuji Cailiao Xuebao/Journal of Inorganic Materials, 2011, 26, 458-466.	1.3	2
118	Photocatalysts based on polymeric carbon nitride for solar-to-fuel conversion. Interface Science and Technology, 2020, 31, 475-507.	3.3	2
119	Spectroscopy Applied to Engineering Materials. Journal of Spectroscopy, 2015, 2015, 1-2.	1.3	1
120	Development and Fabrication of Advanced Materials for Energy and Environment Applications 2014. Journal of Nanomaterials, 2014, 2014, 1-2.	2.7	0